Understanding the Hygroscopic Properties of Supersaturated Droplets of Metal and Ammonium Sulfate Solutions Using Raman Spectroscopy

Yun-Hong Zhang and Chak K. Chan*

Department of Chemical Engineering, Hong Kong University of Science and Technology, Clear Water Bay, Kowloon, Hong Kong

Received: July 12, 2001; In Final Form: October 30, 2001

The hygroscopic properties of sulfate-containing particles are important to understanding the behavior of atmospheric aerosols. At high concentrations, chemical interactions between sulfate ions with the countercations are significant and lead to the formation of contact pairs. In this paper, Raman spectroscopy was used to study the structural changes of single aqueous droplets of equal molar $Na_2SO_4/MgSO_4$ mixture, Na_2SO_4, $(NH_4)_2SO_4$, $MgSO_4$, $ZnSO_4$, and $CdSO_4$ in relation to their hygroscopic properties in an electrodynamic balance. The molar water-to-solute ratio (WSR) and the Raman spectra of droplets equilibrated at different ambient relative humidities were measured. When RH is reduced, the WSR of the $Na_2SO_4/MgSO_4$ droplet decreases from 25.3 to 4.2 without crystallization but with two distinct transition points. The first one appears at WSR = 18.9, where the WSR is more sensitive to RH and the shoulder at 995 cm^{-1} of the ν_1-SO_4^{2-} band of the Raman spectrum shows an abrupt change in the ratio of the intensity at 995 cm^{-1} to that at 984 cm^{-1}. This WSR is close to the minimum ratio (18) required to support the hexaaquo structures for both Mg^{2+} and Na^+ ions. A mixture of the contact ion pairs of $Mg^{2+}O_{6-x}(SO_4^{2-})O_x(H_2O)\cdot Na^+O_{6-y}(SO_4^{2-})O_y(H_2O)$ ($y < x < 6$), which change the spectral characteristic of the shoulder at 995 cm^{-1}, is formed. These contact ion pair mixtures share sulfate ions and water molecules, which invalidate empirical mixing rules of water activity of atmospheric aerosols such as the ZSR model. As RH is further reduced, the second transition point appears at WSR = 7.7, where the WSR becomes almost insensitive to RH and another shoulder at 1002 cm^{-1} appears in the spectrum. The mixture of the contact ion pairs finally evolves into the double salt of $MgSO_4\cdot Na_2SO_4\cdot 4H_2O$, giving two new Raman peaks at 1007 and 1043 cm^{-1}. Transitions of the hygroscopic properties coinciding with the formation of monodentates were also observed for $MgSO_4$ and $ZnSO_4$ droplets.

Introduction

Sulfate is ubiquitously present in atmospheric aerosols. Atmospheric sulfate particles are hygroscopic. In the fine mode sulfate is usually associated with ammonium and nitrate. In the coarse mode, it can be associated with seasalt and crustal ions. Research attention on the hygrosopic properties of atmospheric aerosols has been focused on mixtures of ammonium, sulfate and nitrate,[1−5] and mixtures of sodium, magnesium, and sulfate salts.[6,7] Recently, Chan and Ha[7] measured the water activities of evaporating droplets of mixed salts of Na and Mg with an Electrodynamic Balance (EDB). They found that the ZSR (Zdanovskii−Stokes−Robinson) and the KM (Kusik and Meissner) models give accurate predictions for all Na/Mg systems they studied ($NaCl/MgCl_2$, $NaNO_3/Mg(NO_3)_2$, $NaCl/Mg(NO_3)_2$, $NaCl/MgSO_4$, and $NaNO_3/MgSO_4$) except $Na_2SO_4/MgSO_4$.[7] Using an EDB to study the drying of ceramic precursor droplets, Chan et al.[8] observed an abrupt and significant reduction in the evaporation rate of most zirconium salts and some magnesium salts including magnesium sulfate and magnesium acetate at high concentrations. Chan et al.[7] also found that $MgSO_4$ and $Na_2SO_4/MgSO_4$ mixtures exhibit a significant delay in water evaporation at high concentrations. Such delay was not found in the other systems they studied including the nitrates, chlorides, and sulfates of sodium and ammonium and their mixtures[7,9,10] and the chloride and nitrate of magnesium and their mixtures with sodium salts.[6,7]

Unlike typical electrolytes such as NaCl and $(NH_4)_2SO_4$, $MgSO_4$ does not effloresce at low RH in single particle experiments. Gel formation in concentrated $MgSO_4$ solutions has been postulated to explain the significant reduction in evaporation rate at high concentrations and the inhibition of crystalization.[8,11] Growth measurements of $MgSO_4$ particles also show significant mass transfer limitations at low RH (unpublished data). These special characteristics of $MgSO_4$ droplets have prompted us to study the molecular structures of levitated diluted and supersaturated $(NH_4)_2SO_4$ and $MgSO_4$ droplets using Raman spectroscopy.[11] A significant shift of the ν_1-SO_4^{2-} band from 983 to 1007 cm^{-1} and an increase of its full width at half height (fwhh) from 12 to 54 cm^{-1} were observed when the molar water-to-solute ratio (WSR) decreased from 17.4 to 1.5. Such spectral changes have been attributed to the formation of contact ion pairs of Mg^{2+} and SO_4^{2-} in supersaturated droplets of $MgSO_4$ at WSR smaller than 6, where there are insufficient water molecules to maintain the hexaaquo structure of fully hydrated Mg^{2+}. In these contact pairs, Mg^{2+} and SO_4^{2-} are bonded without water molecules between the ions. These contact pairs include monodentate and bidentate, which can form a chain structure incorporating water, inhibiting mass transfer and suppressing crystallization. Contact pairs of NH_4^+ and SO_4^{2-} exist at WRS between 3.9 and 1.5, but the interactions are weak

* Corresponding author. E-mail:keckchan@ust.hk. Phone: (852) 2358-7124. Fax: (852) 2358-0054.

10.1021/jp012694j CCC: $22.00
Published on Web 12/18/2001

CHART 1: Structures of Contact Ion Pairs between Sulfate and Metal Cations

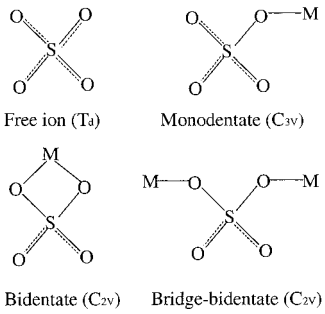

and result only in a little red shift of the ν_1-SO_4^{2-} band from 981 to 977 cm^{-1}.

The formation of contact ion pairs in aqueous sulfate salt solutions has been associated to the crystal growth of double sulfate salts, such as $LiASO_4$ (A = Na, K, Rh, Ag, etc.), which have applications in ionic conductors and ferroelectric materials.[12−14] Classical experimental methods such as freezing point measurements, potentiometric measurements, ultrasonic absorption, and solubility measurements, which measure the macrophysical bulk properties of solutions in which the contact ion pairs may exist, cannot yield direct information about contact ion pairs at the molecular level.[15−19] Although there are many studies on the equilibrium distributions of free ions, outer sphere ion pairs, outer−inner ion pairs and contact ion pairs in salt solutions in the literature, there has not yet been an agreement on the association constants of sulfate salts such as $MgSO_4$, $ZnSO_4$ and $CdSO_4$, especially those at higher concentrations.[20,21] Sulfate has been found to be coordinated with metal ions in the form of monodentate, bidentate as well as bridge-bidentate forms in solid sulfate salts, as shown in Chart 1.[22−26] Spectroscopic techniques, including Raman scattering, infrared spectroscopy, and NMR, provide information about contact ion pairs on a molecular level.[27−36] However, most of the studies are limited to diluted concentrations because of the constraints of saturation in bulk samples. By using an electrodynamic balance in which single supersaturated droplets were levitated in an electric field, we found that both monodentate and dibentate exist in supersaturated $MgSO_4$ droplets.[11] Bidentate contact ion pairs of a series of anionic complexes from $[M(SO_4)_2]^{2-}$ to $[M(SO_4)_5]^{8-}$ (M = Zn(II) or Cd(II)) in their bulk solutions have been proposed by Fedorov et al.[37,38] There are also some reports on the theoretical calculations of the structures of contact ion pairs, but they are all focused on monodentates.[20]

In this paper, we extend our earlier work of Raman characterization of levitated droplets of $MgSO_4$ to Na_2SO_4/$MgSO_4$, a system in which strong molecular interactions between the ions are expected based on the significant mass transfer effects in the hygroscopic measurements observed earlier by our group.[7] In particular, the hygroscopic properties and the Raman spectra of the Na_2SO_4/$MgSO_4$ droplets, will be compared with $(NH_4)_2SO_4$, $MgSO_4$, $ZnSO_4$, and $CdSO_4$ droplets. Although the last two sulfate systems have less atmospheric significance, a large body of literature on their spectroscopic properties is available for comparison. The ultimate aim of this study is to understand the hygroscopic properties of the metal sulfate systems at high concentrations at molecular levels using Raman spectroscopy. The formation of contact pairs in these systems will also be discussed.

Experimental Section

Since a droplet is freely levitated in an electric field in an electrodynamic balance (EDB), heterogeneous nucleation is suppressed and therefore supersaturated droplets can be studied. Many thermodynamic studies of supersaturated solutions of inorganic salts using an EDB have been reported. In addition to the study of contact pairs, the phase transformation and metastability of supersaturated microparticles can be studied by combining an EDB system with a Raman spectroscopic system.[39,40] Other applications of single particle Raman spectroscopy include studies of transport properties and chemical reactions of suspended aerosols.[41−45]

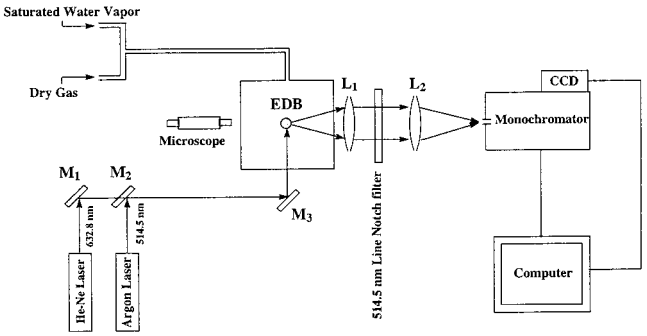

Figure 1. The schematic of an EDB − Raman system.

The experimental setup and procedures used in this study are identical to those used in Zhang and Chan.[11] Figure 1 shows the schematic diagram of the apparatus for the water cycle and Raman scattering measurements of levitated droplets. A charged single droplet, illuminated by a He−Ne laser and observed by a 20× microscope, was held stationary at the center in the EDB. The relative humidity in the EDB was adjusted by mixing a stream of saturated air and another of dry air at controlled flowrates. The dew point of the gas was measured by a hygrometer (EG&G Dew Prime Model 2000). At equilibrium the water activity of the droplet is related to the ambient relative humidity (RH_1) by $a_w = P_w/P_w^{sat} = RH_1/100$. The DC voltage ($DC_1$) was adjusted so that the weight of the droplet balanced the electrostatic force it experienced. The DC_1 value is related to the mass fraction of solute (mfs_1) of the droplet by $mfs_1 = mfs_0DC_1/DC_0$, where DC_0 and mfs_0 are the values at a particular reference state, such as the saturation point (RH = 84%; mfs_0 = 0.362) of bloedite for the 1:1 Na_2SO_4/$MgSO_4$ droplet. The water-to-solute ratio (WSR) of the droplet is $W(1 - mfs)/(18mfs)$, where W is the molecular weight of the sulfate salt. For the 1:1 Na_2SO_4/$MgSO_4$ droplets, W is the sum of the molecular weight of the two components. The size of the droplets studied was about 30−60 μm. The water activities of the bulk solutions were measured by an AquaLab water activity meter (model series III, Decagon Device, Inc).

In the Raman measurements, a 5 W argon ion laser (Coherent I90-5) was used as an excitation source. The output power of the 514.5 nm excitation line was between 800 and 1000 mW. A 0.5m monochromator (Acton SpectraPro 500) attached to a CCD (Princeton Instruments, TE/CCD-1100PFUV) detector was used. A 1200 g/mm grating of the monochromator was selected. A pair of lenses, which matches the f/6.9 optics of the monochromator, was used to focus the 90° scattering of the levitated droplet to the slit of the monochromator. A 514.5 nm Raman notch filter was placed between the two lenses to remove the strong Rayleigh scattering. The resolution of the spectra obtained was 2.3 cm^{-1} at 981 cm^{-1}. The spectra reported in this work were the averages of the 30 frames, each with an accumulation time of 5 s. All measurements were made at ambient temperatures of 22−24 °C.

Morphological resonances in Mie scattering sometimes complicate the Raman spectra of droplets. There are two types

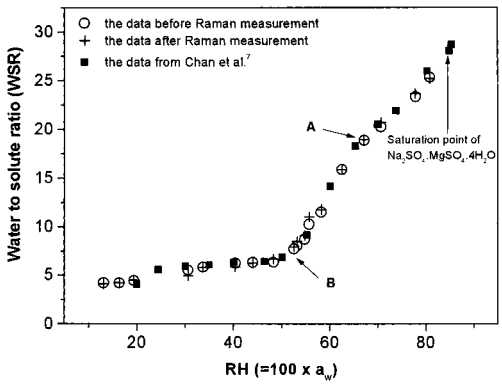

Figure 2. The water to solute molar ratios of 1:1 $Na_2SO_4/MgSO_4$ droplets as a function of RH.

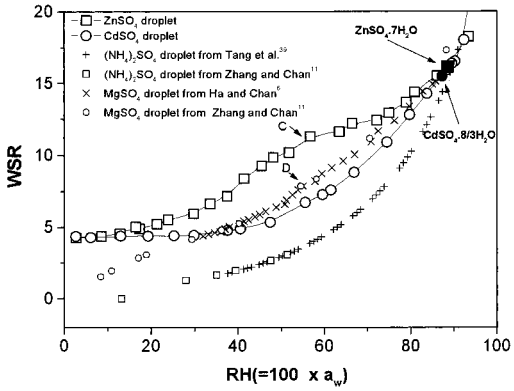

Figure 3. Molar water-to-solute ratio of $ZnSO_4$, $CdSO_4$, $(NH_4)_2SO_4$, and $MgSO_4$ droplets at various ambient RH.

of morphological resonance effects. The first type is that the excitation wavelength is at a resonance wavelength and scattering (elastic and Raman) signals at all wavelengths are enhanced. This type of resonance does not affect our analysis. The second type is that the Raman emissions at selected wavelengths are at resonance, which complicate the analysis of the molecular changes of the droplets. To reduce the effect of the resonance on the Raman scattering, we used relatively large droplets from 30 to 60 micron in diameter. Generally, the morphological resonances have sharp peaks with fwhh of 1−5 cm^{-1}. For dilute droplets, it is difficult to differentiate these resonance peaks from the true Raman peaks because the fwhh of $\nu_1-SO_4^{2-}$ is about 10 cm^{-1}, close to that of the resonance peaks. However, in the supersaturated droplets, the fwhhs of the Raman peaks of $\nu_1-SO_4^{2-}$ of $MgSO_4$, $ZnSO_4$, and the mixture $MgSO_4/Na_2SO_4$ are much wider (30−60 cm^{-1}). At each RH, over 50 Raman spectra of the droplet were measured. The spectra affected by the resonance effects were identified and excluded from our analysis. The reported spectra are the averages from those not affected by the morphological resonance.

Raman spectra of bulk solutions and solid samples were measured using a Renishaw 3000 micro-Raman system with an Olympus BH-2 microscope at 20× magnification. The excitation source used was a helium−neon laser operating at 632.8 nm with an output power of 25 mW. The spectral resolution was approximately 1.0 cm^{-1}.

Results

1. The Molar Water-to-Solute Ratio (WSR) of Sulfate Droplets. Figure 2 shows the hygroscopic properties of equal molar $Na_2SO_4/MgSO_4$ droplets before (plus) and after (open circle) each Raman measurement, in terms of the equilibrium WSR as a function of decreasing RH. The saturation point (a_w = 0.84; WSR = 25.75) of the double salt $Na_2SO_4.MgSO_4{\cdot}4H_2O$ (bloedite) was used as the reference state for calculating the WSR at other RH.[46] The data are consistent with Chan et al. [7] (solid square). It can be seen that the Raman measurements did not affect the hygroscopic properties of the droplets. Efflorescence, which would lead to a sudden decrease in the WSR, was not observed even at RH = 13%. The addition of $MgSO_4$ suppressed the crystallization of Na_2SO_4, which occurred at RH = 55%−57% in levitated aqueous Na_2SO_4 droplets.[9−10]

Starting at RH = 80.8%, the WSR decreases as the RH decreases. A transition point (A in Figure 2) appears at a WSR of about 18.9 (at RH = 67%), where the WSR becomes more sensitive to RH until the ratio reaches about 7.7 (at RH = 52.6%; point B). As the RH continues to decrease to below 52.6%, the WSR changes only slightly and the droplet approaches a stoichiometry of a $Na_2SO_4.MgSO_4{\cdot}4H_2O$ without crystallization. The particle remains spherical at low RH as observed through the microscope. Considering that there are six water molecules in the first-full-layer of each sodium ion[47−49] and magnesium ion,[50,51] 18 H_2O molecules are needed to be shared by one Mg^{2+} and two Na^+ ions. Contact ion pairs should start to form at WSR = 18 and below, close to the first transition point (A) observed in Figure 2. In next section, we will discuss the spectral evidence of the formation of contact ion pairs.

The WSR of $ZnSO_4$ and $CdSO_4$ droplets as a function of RH is shown in Figure 3. Bulk saturated solutions of $ZnSO_4{\cdot}7H_2O$ (a_w = 0.90; WSR = 16.08)[52,53] and of $CdSO_4{\cdot}8/3H_2O$ (at a_w = 0.889 and WSR = 15.16) were chosen as reference states. Literature reports on $MgSO_4$ and $(NH_4)_2SO_4$ solutions are also shown for comparison.[11,39] The WSR of $ZnSO_4$ droplets decreases continuously when RH decreases. Similar to 1:1 $Na_2SO_4/MgSO_4$ droplets, a transition point (point C in Figure 3) exists near RH = 56.7%. Between RH = 56.7% and 24%, the ratio decreases steeply from 11.3 to 5.5. At RH below 24%, the ratio is relatively insensitive to RH. Albeit less obvious, there is also a transition point (point D in Figure 3) of the data of $MgSO_4$ droplet. The WSR of the $CdSO_4$ droplet decreases continuously from 16.4 to 5.4 when RH decreases from 90% to 47%. As the RH further decreases, the ratio slightly decreases from 5.4 to 4.5. No obvious transition point of the data was observed for $CdSO_4$ droplets.

Except for $(NH_4)_2SO_4$, all sulfate systems we studied do not crystallize. The lowest WSR achieved was 1.7, 1.5, 4.2, 4.3, and 4.5 for $(NH_4)_2SO_4$, $MgSO_4$, $Na_2SO_4/MgSO_4$, $ZnSO_4$, and $CdSO_4$ droplets, respectively. Such low WSR facilitates the formation of contact pairs, resulting in changes of the symmetric stretching vibration band of SO_4^{2-} (ν_1-SO_4^{2-}) at 980−983 cm^{-1} of the Raman spectra.

2. Raman Spectra of the Dilute Droplets. There are many Raman studies of the contact ion pairs of sulfate salts in the literature. Free SO_4^{2-} ions have T_d symmetry and nine modes of internal vibration spanning the representation $\Gamma_{vib} = A_1 + E + 2F_2$. All modes are Raman active, but only the F_2 modes are IR active. The symmetric stretching vibration band of SO_4^{2-} (ν_1-SO_4^{2-}) appears in the range of 980−983 cm^{-1}, whose detailed characteristics of peak location and fwhh, are sensitive to the countercation species, the salt concentration, and temperature.[20,21,27−36,54−56] We have recently reported the appearance of a shoulder at 995 cm^{-1} when monodentate contact ion pairs are formed in concentrated $MgSO_4$ solutions.[11] The corresponding shoulders of $ZnSO_4$ and $CdSO_4$ solutions have been resolved at 987 and 989 cm^{-1}, respectively.[20,54] Figure 4

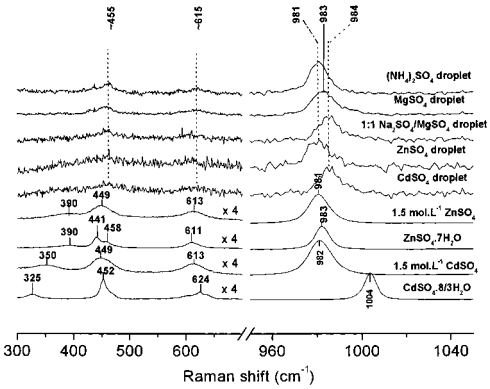

Figure 4. Raman spectra of dilute solution droplets of the sulfate systems studied.

shows that the Raman spectra of dilute $(NH_4)_2SO_4$, $MgSO_4$, 1:1 $Na_2SO_4/MgSO_4$, $ZnSO_4$, and $CdSO_4$ droplets (at WSR of 15.8, 17.4, 25.3, 18.2, and 16.4) have the ν_1-SO_4^{2-} bands at 981, 983, 984, 981, and 984 cm^{-1}, respectively. The ν_1-SO_4^{2-} bands of 1.5 mol L^{-1} (WSR = 37) bulk $ZnSO_4$ and $CdSO_4$ solutions appear at 981 and 982 cm^{-1}, while those of $ZnSO_4 \cdot 7H_2O$ crystal and $CdSO_4 \cdot 8/3H_2O$ crystal appear at 983 and 1004 cm^{-1}. Slight asymmetries on the high-frequency side of the ν_1-SO_4^{2-} band were observed for diluted $MgSO_4$, 1:1 $Na_2SO_4/MgSO_4$, $ZnSO_4$, and $CdSO_4$ droplets but were not seen in $(NH_4)_2SO_4$ solutions.[11]

The stretching mode of M−O−$(H_2O)_6$ (M = Mg^{2+}, Zn^{2+}, or Cd^{2+}) has been observed by Rudolph et al.[20,29,54] In Figure 4, this mode appears at 390 and 350 cm^{-1} for bulk $ZnSO_4$ and $CdSO_4$ aqueous solutions, respectively. However, it was not observed in the droplet spectra because its intensity was very weak. It is interesting to note that $ZnSO_4 \cdot 7H_2O$ solid has a peak at 390 cm^{-1}, similar to its bulk aqueous solution while $CdSO_4 \cdot 8/3H_2O$ solid has a large blue shift from 350 to 325 cm^{-1} when compared with its bulk aqueous solution.

3. Raman Spectra of Concentrated Sulfate Droplets. The most direct approach to investigating the formation of contact ion pairs is to obtain the vibration spectra of the bond between two partners. However, the strong quasi-elastic Rayleigh wing, extending to 500 cm^{-1}, complicates the detection of the weak low-frequency modes of the metal−sulfate bond. Using the difference spectroscopy method to obtain spectral information in the low-frequency region of the peak of contact ion pairs, Rudolph et al.[20,29,32−35,54] have obtained significant findings on the contact ion pairs of sulfate salt solutions. In particular, they resolved a band at 240 cm^{-1} from the Cd(II)-O stretching vibration mode of the hexaaquo complex near 350 cm^{-1} and assigned it to the Cd(II)−O stretching vibration of Cd(II)−O−SO_3^{2-} in bulk $CdSO_4$ solutions.[20] The Mg^{2+}−O(SO_4^{2-}) and Zn^{2+}−O(SO_4^{2-}) stretching vibration bands were resolved at 245 and 275 cm^{-1}, respectively.[20,29,54] In our study, the Raman signals of the droplets were too weak for the observation of these bands as mentioned above. Even though the two bending modes and the anti-symmetric stretching mode were seen near 455, 615 and 1120 cm^{-1}, their intensities and the signal-to-noise ratios were too low to provide useful information on the formation on contact ion pairs. Instead, the ν_1-SO_4^{2-} band characteristic is sensitive to the strong interactions between the metal and sulfate ions and therefore it provides much information on the contact ion pairs.

Figure 5a−e show the ν_1-SO_4^{2-} bands of (a) $(NH_4)_2SO_4$, (b) $MgSO_4$, (c) 1:1 $Na_2SO_4/MgSO_4$, (d) $ZnSO_4$, and (e) $CdSO_4$ droplets at various WSR. The aqueous $(NH_4)_2SO_4$ solution is usually considered to be a model of "free" sulfate systems. The

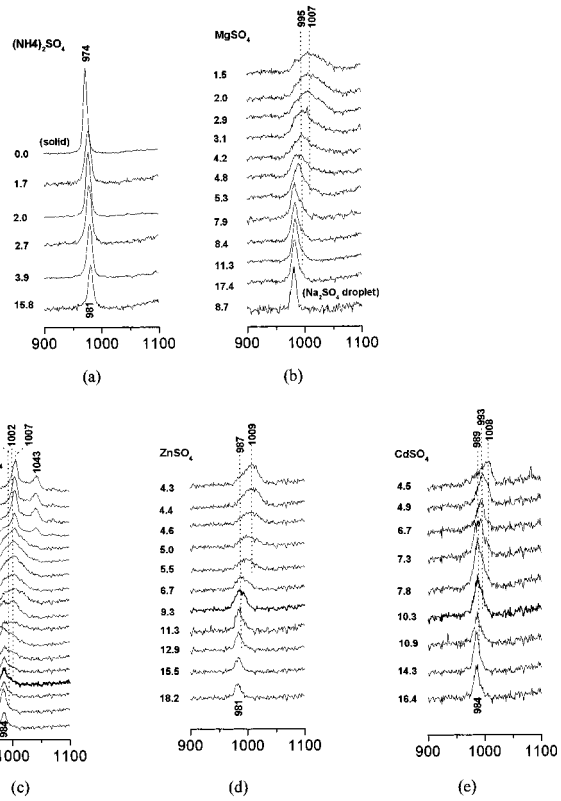

Figure 5. Raman spectra of (a) $(NH_4)_2SO_4$, (b) $MgSO_4$, (c) 1:1 $Na_2SO_4/MgSO_4$, (d) $ZnSO_4$, and (e) $CdSO_4$ droplets at various molar water-to-solute ratios.

ν_1-SO_4^{2-} band of $(NH_4)_2SO_4$ droplets has only a small red shift from 981 to 977 cm^{-1} when the WSR decreases from 15.8 to 1.7 (Figure 5a). $MgSO_4$ droplets (Figure 5b), however, have a significant blue shift from 983 to 1007 cm^{-1} and an increase of the fwhh from 12 to 54 cm^{-1} of the ν_1-SO_4^{2-} band when the WSR decreases from 17.4 to 1.5. Such spectral changes have been assigned to the formation of the contact ion pairs with structures of monodentate and bidentate in highly supersaturated solutions.[11] The asymmetry of the ν_1-SO_4^{2-} band at high WSR (17.4−8.4) is attributed to the presence of a shoulder at 995 cm^{-1}, which has been associated to the formation of the monodentate contact ion pair between Mg^{2+} and SO_4^{2-}. This shoulder becomes a peak at WSR = 5.3. As the WSR further decreases, another peak at 1007 cm^{-1} emerges, probably due to the formation of bidentates.

The evolution of the spectrum of $Na_2SO_4/MgSO_4$ droplets (Figure 5c) is complex. At high WSR (>23), a shoulder appears at 995 cm^{-1}. This shoulder grows as WSR decreases. The growth becomes more pronounced at WSR = 18.9. This WSR corresponds to the transition point A of the water activity data shown in Figure 2. As the WSR further decreases, another shoulder at about 1002 cm^{-1} begins to emerge. The intensities of the two shoulders increase simultaneously until WSR = 8.7, where the shoulder at 1002 cm^{-1} becomes a peak. At WSR below 5.5, two new peaks at 1007 and 1043 cm^{-1} appear.

The Raman spectra of $ZnSO_4$ droplets (Figure 5d) show that the "free" ν_1-SO_4^{2-} band is resolved at 981 cm^{-1}, which includes free SO_4^{2-} ions as well as the outer−outer ion pairs and outer-inner ion pairs as proposed by Rudolph et al.,[20,54] and remains a main peak until WSR reaches 9.3. At WSR between 9.3 and 6.7, the droplet is rich in monodentate, as evidenced by the presence of the shoulder at 987 cm^{-1}. As the WSR further decreases to 4.3, a peak near 1009 cm^{-1} gradually evolves.

A shoulder corresponding to the monodentate contact ion pair of $CdSO_4$ has been observed at 989 cm^{-1}.[20] As shown in Figure 5e, this shoulder becomes a main peak when WSR is between 10.3 and 7.8. Another shoulder at 993 cm^{-1} evolves into a main peak at a ratio between 6.7 and 4.9. Finally, a third shoulder at 1008 cm^{-1} emerges at WSR = 4.9 and becomes a main peak at WSR = 4.5

Discussion

As shown in Figure 5, asymmetry in the ν_1-SO_4^{2-} band was observed in all diluted droplets of the metal sulfate systems studied except $(NH_4)_2SO_4$. Similar asymmetry has been reported for most metal sulfate bulk solutions.[27−36] The cause of the asymmetry of the ν_1-SO_4^{2-} band has been a controversial issue in the literature. Some researchers[21,55,56] attributed it to the change of the local potential field experienced by the sulfate ion because of the interactions with hydration water or the electrostatic interactions with the counterion, while others[20,27,29,34,35] argued that the presence of the shoulder peak at 995 cm^{-1}, which causes the asymmetry, is an indicator of the presence of the contact ion pairs in $MgSO_4$ aqueous solutions. This uncertainty has arisen partially because of the small population of contact ion pairs in dilute or even saturated solutions in bulk solutions, thus limiting the intensity of the shoulder in the spectra. The limitation was relaxed by studying highly supersaturated droplets in this study. Although the signal-to-noise ratio of the Raman scattering of the supersaturated droplets shown in Figure 5 is not as good as those of bulk solutions, the spectral characteristic of the ν_1-SO_4^{2-} band provides clear evidence of the presence of the contact ion pairs of different structures in these highly concentrated (supersaturated) droplets. We have observed that the shoulder at 995 cm^{-1} develops into a main peak and the fwhh shows an abrupt increase when the WSR of $MgSO_4$ droplets decreases to below 6, where Mg^{2+} and SO_4^{2-} ions form direct contact ion pairs to maintain the six coordination structure.[11] The increase of fwhh values in these supersaturated droplets is an indication of the presence of contact ion pairs of different structures, which is also the reason for the difficulty in determining the association constants of the contact pairs.[20−21]

Although it is difficult to conduct a quantitative analysis on the composition distribution of the contact pairs, the intensity ratio of the signals of the peak at 995 cm^{-1} and the free ν_1-SO_4^{2-} peak at 983 cm^{-1} (I_{995}/I_{983}) can be used as an indicator for the relative abundance of monodentate and the "free" sulfate ions, especially in the initial process of the formation of contact ion pairs. Figure 6a summarizes the results of hygroscopic and Raman measurements of $MgSO_4$ droplets in the form of RH and I_{995}/I_{983} as a function of WSR. It is very interesting to note that, as WSR decreases, an abrupt increase of I_{995}/I_{983} appears at WSR = 7.9, the transition point D shown in Figure 3. Hence, the change of the hygroscopic property of $MgSO_4$ droplets is related to the formation of monodentate contact ion pairs.

In general, Na_2SO_4 is assumed to be completely dissociative in water,[57−59] although there are reports on the formation of $NaSO_4^-$ ion pairs.[60−63] In particular, Daly et al. reported Raman spectra of the contact ion pair between Na^+ and HSO_4^- ions.[63] On the other hand, Rull et al. studied the dependence of the dynamics of SO_4^{2-} ions in Li_2SO_4, Na_2SO_4, and K_2SO_4 aqueous solutions on the solution concentration and temperature.[64] They found that the fine asymmetry of the ν_1-SO_4^{2-} band was dependent on the nature of the cation species and they explained the dependence by the perturbation of the cations on the dynamics of the water molecules around the SO_4^{2-} ions rather than by the formation of contact ion pairs.

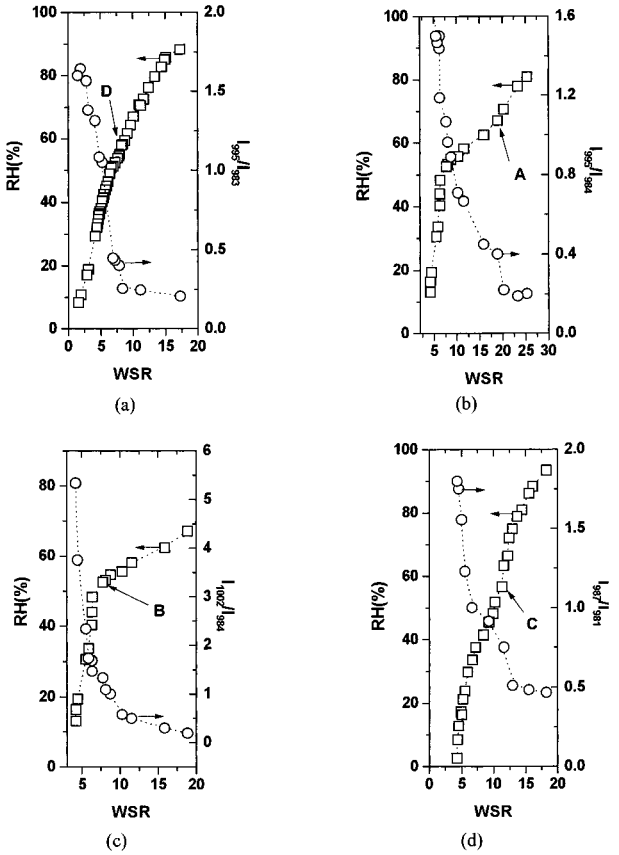

Figure 6. (a) I_{995}/I_{983} vs WSR of $MgSO_4$. (b) I_{995}/I_{984} vs WSR of 1:1 Na_2SO_4/ $MgSO_4$. (c) I_{1002}/I_{984} vs WSR of 1:1 Na_2SO_4/$MgSO_4$. (d) I_{987}/I_{981} vs WSR of $ZnSO_4$ droplets.

Similar to $MgSO_4$ droplets, the WSR of Na_2SO_4 droplets was reduced to below the minimum value (WSR = 12) required to form a hydrated-inner-sphere structure so that contact pairs can be formed. However, as shown in Figure 5b (the bottom spectrum), no obvious change of the ν_1-SO_4^{2-} band was observed from Na_2SO_4 droplets at WSR = 8.7.

Crystallization of Na_2SO_4/$MgSO_4$ droplets was not observed even at WSR as low as 4.2. Figure 6b shows that the intensity ratio of the signals at 995 and 984 cm^{-1} of the ν_1-SO_4^{2-} band (I_{995}/I_{984}) starts to increase when WSR decreases to 18.9. This WSR ratio is close to the minimum value (WSR = 18) required to maintain the hexaaquo structures for all Mg^{2+} and Na^+ ions. Thus, the transition point A in Figure 2 can also be explained by the formation of contact ion pairs giving rise to the shoulder at 995 cm^{-1}. The experimental water activity data of Na_2SO_4/$MgSO_4$ droplets are not consistent with the predictions of simple mixing rules such as the ZSR and the KM models, which work well for other Na/Mg systems studied with an electrodynamic balance. Thus, the contact ion pair mixtures that give rise to the shoulder do not merely consist of simple noninteracting mixtures of [$MgSO_4$] and [$NaSO_4^-$] contact ion pairs. Instead, the increase of I_{995}/I_{984} when WSR decreases from 18.9 can be explained by the formation of a mixture of $Mg^{2+}O_{6-x}(SO_4^{2-})O_x$-$(H_2O)\cdot Na^+O_{6-y}(SO_4^{2-})O_y\cdot(H_2O)$, where the $(6 - x)$ oxygen atoms associated with magnesium ions and the $(6 - y)$ oxygen atoms associated with sodium ions are from sulfate ions and the other oxygen atoms (O_x and O_y) are from water molecules. Because Mg^{2+} (−1922.1 kJ.mol^{-1}) has a higher hydration energy than that of Na^+ (−405.4 kJ.mol^{-1}),[65] the contact ion pairs between Na^+ and SO_4^{2-} should be the first to form in this mixed system at WSR = 18.9, i.e., $y < x < 6$, although the contact ion pairs between Na^+ and SO_4^{2-} have little effect

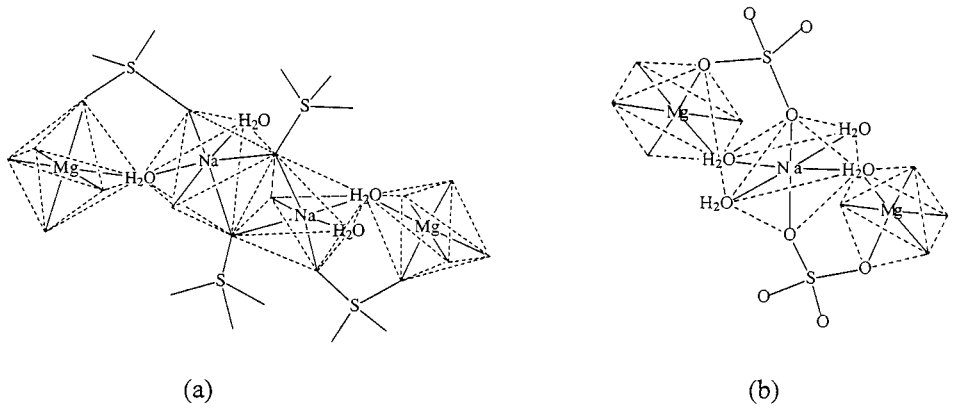

(a) (b)

Figure 7. (a) The crystal structure of the bloedite and (b) a possible structure of a mixture contact ion pair in the supersaturated droplet of 1:1$Na_2SO_4/MgSO_4$.

TABLE 1: Hydration Properties of the Metal Cations

parameters	Na^+	Mg^{2+}	Zn^{2+}	Cd^{2+}
ionic radius (Å)[65]	0.95	0.65	0.74	0.97
distance of M−O $(H_2O)_6$ (Å)	2.40−2.50[69d]	2.00−2.15[69f]	2.08−2.15[67b]	2.29−2.31[69a,b]
hydration energy(kJ mol^{-1}) [65]	−405.4	−1922.1	−2044.3	−2384.9
ν-M−O$(SO_4^{2-})(H_2O)_5$ (cm^{-1})[20,29,54]		245	275	240

on the ν_1-SO_4^{2-} band as shown in Figure 5b (bottom spectrum). This is consistent with the structure of the double salt of $Na_2SO_4{\cdot}MgSO_4{\cdot}4H_2O$ in which $x = 4$ and $y = 2$.[66] In these Na−$MgSO_4$ contact pairs, the Na and the Mg contact pairs are connected by sharing a sulfate and a water molecule. It is therefore not surprising that empirical models such as the ZSR and KM models, which assume no chemical interactions between the different solutes, give poor predictions of this system.

Figure 6c shows that the intensity ratio of the signals at 1002 and at 984 cm^{-1} (I_{1002}/I_{984}) exhibits an abrupt increase as WSR decreases to 7.7, which is the second transition point B in Figure 2, where the WSR becomes much less sensitive to further decreases in RH.

At saturation, the double salt of $Na_2SO_4{\cdot}MgSO_4{\cdot}4H_2O$ is formed from equal molar Na_2SO_4−$MgSO_4$ bulk solutions.[46] As shown in Figure 2, the WSR remains approximately constant at 4 at RH < 20%, which is also consistent with the observation by Chan et al.[7] The droplet at low RH has a stoichiometry of $Na_2SO_4.MgSO_4{\cdot}4H_2O$ without crystallization. Hence the particle may be in the less thermodynamically stable amorphous state. Mass transfer limitations may have suppressed the delay of crystallization. Nevertheless, two peaks at 1007 and 1043 cm^{-1} in Figure 5c can be assigned to the tetraaquo double salt**.**

The structure of the double salt has been described in terms of layers built up by $MgO_2(H_2O)_4$ and $NaO_4(H_2O)_2$ octahedra lying on the (001) planes.[66] These layers contain infinite chains of alternating $MgO_2(H_2O)_4$ and $NaO_4(H_2O)_2$ sharing corners and pairs of $NaO_4(H_2O)_2$ octahedra sharing one edge, as shown in Figure 7a. Adjacent octahedral layers are interconnected by SO_4 tetrahedra. Similar to the double salt structure, a structure consisting of one magnesium ion bridge connecting with a sodium ion by a sulfate ion or a water molecule can also form a chain. Figure 7b shows an example of such a structure of a mixture of contact ion pairs. The formation of such a chain can possibly explain the observation of significant reduction of the mass transfer rates in the drying experiments made by Chan et al.[7]

$[Zn(H_2O)_6]^{2+}$ has been observed with non-coordinating anions such as nitrate, sulfate in many aqueous solutions[67] and even in crystals.[68] For example, a $ZnSO_4{\cdot}7H_2O$ solid with octahedral $[Zn(H_2O)_6]^{2+}$ unit is well-known.[68e] The hexaaquo Zn(II) complex obstructs the direct contact between SO_4^{2-} and Zn^{2+}. Thus, the ν_1-SO_4^{2-} band of the $ZnSO_4{\cdot}7H_2O$ solid appears at 983 cm^{-1}, similar to that found in its aqueous solution shown in Figure 4. A similar conclusion can be made for the ν-Zn^{2+}−$O(H_2O)_6$ peak at 390 cm^{-1} in the spectra of both $ZnSO_4{\cdot}7H_2O$ solid and its bulk solution.

In Figure 6d, an abrupt change of I_{987}/I_{981} in $ZnSO_4$ droplets occurs when the WSR decreases to 11.3. This is the transition point C shown in Figure 3. Although such a molar ratio is sufficient for each zinc ion to maintain a hexaaquo $[Zn(H_2O)_6]^{2+}$ complex in the droplet, it appears that a large number of monodentate contact ion pairs exist. Other kinds of contact ion pairs, possibly bidendate or bridge-bidentate contact ion pairs corresponding to the peak at 1009 cm^{-1}, are formed gradually when WSR further decreases as shown in Figure 5d.

Octahedral $[Cd(H_2O)_6]^{2+}$ has been observed in both aqueous solutions and in solid $Cd(ClO_4)_2{\cdot}6H_2O$.[69a,b] In our experiments, monodentate contact ion pairs exist at WSR between 10.3 and 7.8, based on the intensities at 989 and 984 cm^{-1}.[12,54] There are two shoulders beside the shoulder at 989 cm^{-1} corresponding to the monodentate contact ion pairs. These two shoulders develop into a major peak at lower WSR, indicating the presence of contact ion pairs other than the monodentate. For example, the shoulder at 993 cm^{-1} becomes a major peak at WSR of 6.7 to 4.9, which is probably from the bidentate contact ion pairs. Another peak at 1008 cm^{-1} may be related to anionic complexes.[37,38]

As discussed above, unlike in $MgSO_4$ and $Na_2SO_4/MgSO_4$ droplets, both the monodentate and bidentate contact ion pairs are formed in $ZnSO_4$ and $CdSO_4$ droplets at a WSR higher than 6, the minimum number to maintain the full hydrated inner-sphere of the cations. In general, the interaction between the second-layer hydration water molecules and the primary shell water molecules is stronger than that among bulk water molecules because of the polarization effect of cations on the primary shell water molecules. Table 1 lists the ionic radius, the atomic M−O $(H_2O)_6$ distance, the hydration energy and some spectroscopic data of the cations. The polarization effect is proportional to the charge-to-radius ratio of the cations in the following order, namely, $Mg^{2+} > Zn^{2+} > Cd^{2+}$ ($\gg Na^+$).

The contribution of the second and higher layer water molecules to the total hydration energy also follows the same order. On the other hand, the hydration energy of Cd^{2+}, Zn^{2+} and Mg^{2+} are −2384.9, −2044.3, and −1922.1 kJ.mol^{-1}, respectively.[65] Hence, the strength of the interaction between the metal cations and the primary shell water molecules in the hexaaquo complexes decreases in the order of $Cd^{2+} > Zn^{2+} > Mg^{2+}$ ($\gg Na^+$), which is consistent with the trend of the difference of the distance of $M-O(H_2O)_6$ and the ionic radius, according to Table 1. Thus, Cd^{2+} and Zn^{2+} have a higher tendency to remain in their hexaaquo complex structures compared with Mg^{2+}. However, our results show that contact ion pairs are formed at a WSR higher than 6 in $ZnSO_4$ and $CdSO_4$ droplets while they are formed only when there are insufficient water molecules to maintain the primary shell of the hexaaquo complex of Na^+ or Mg^{2+} in $MgSO_4$ and 1:1 $Na_2SO_4/MgSO_4$ droplets. This suggests that the interaction between Cd^{2+} and SO_4^{2-} (and between Zn^{2+} and SO_4^{2-}) in the contact ion pairs must be stronger than that between Mg^{2+} and SO_4^{2-} (and much stronger than that between Na^+ and SO_4^{2-}). This is also supported by the observed frequencies of the $M-O(SO_4^{2-})(H_2O)_5$ stretching vibration, as shown in Table 1. Even though the atomic weight of Zn is much higher than that of Mg, the ν-Zn(II)$-O(SO_4^{2-})(H_2O)_5$ is at 275 cm^{-1}, which is much higher than that of ν-$Mg^{2+}-O(SO_4^{2-})(H_2O)_5$. Considering that the spherically filled 18-e d electron cloud of Cd^{2+} and Zn^{2+} is more easily polarized by anions than the 8-e shell of Na^+ and Mg^{2+}, we propose that the covalent nature of contact ion pairs increases in the following order: $Na^+-SO_4^{2-}$, $Mg^{2+}-SO_4^{2-} < Zn^{2+}-SO_4^{2-}$, $Cd^{2+}-SO_4^{2-}$.

Conclusion

This paper demonstrates how an EDB−Raman system can be used to correlate changes in molecular structures, specifically in the formation of contact ion pairs to the hygroscopic properties of sulfate salts when RH decreases. An EDB−Raman system is a unique combination to measure spectroscopic signatures of contact ion pairs, which may be difficult to detect otherwise. Similar studies can be extended to metal−organic ion systems, which have generated much atmospheric interest recently.

All the monodentate contact ion pairs of the metal sulfates studied were observed when the droplets were in supersaturation states. This observation cannot be achieved in bulk solutions. The spectra of bulk solutions show only a weak shoulder on the higher wavenumber side of ν_1-SO_4^{2-} band for monodentate for most metal sulfate systems. The shoulders are often too weak for molecular assignment. Continuous formation of other forms of contact ion pairs, possibly bidentate and bridge bidentate and even some chain structures, results in the increase of fwhh for $MgSO_4$ and $ZnSO_4$ droplets. Although it is difficult to determine the association constants in the formation of different contact pairs, qualitative analysis of the ratios of the signal intensities (I_{995}/I_{983} for $MgSO_4$, I_{987}/I_{981} for $ZnSO_4$ as well as I_{995}/I_{984} and I_{1002}/I_{984} for 1:1 $Na_2SO_4/MgSO_4$ droplets) is useful to relate the formation of contact ion pairs and the hygroscopic properties of these sulfate systems. In particular, the two transition points of the hygroscopic curve of 1:1 $Na_2SO_4/MgSO_4$ droplet at WSR = 18.9 and 7.7 are related to the abrupt increases of I_{995}/I_{984} and I_{1002}/I_{984}. Although the structures of the contact ion pairs corresponding to 995 and 1002 cm^{-1} shoulders are not well-understood, we propose that they are built up by $Mg^{2+}O_{6-x}(SO_4^{2-})O_x(H_2O)$ and $Na^+O_{6-y}(SO_4^{2-})O_y(H_2O)$ octahedra units sharing water molecules or sulfate ions, similar to the double salt. The $Mg^{2+}O_{6-x}(SO_4^{2-})O_x(H_2O)$ and $Na^+O_{6-y}(SO_4^{2-})O_y(H_2O)$ octahedra units could form some chain structures, which possibly explains the observation of the significant reduction of the mass transfer rates in the drying experiments. A spectroscopic evolution from such mixture of contact ion pairs to the double salts of $Na_2SO_4 \cdot MgSO_4 \cdot 4H_2O$ was also observed with further decrease of WSR. The covalent nature between metal ions and sulfate ions in the contact ion pairs increases in the following order: $Na^+-SO_4^{2-}$, $Mg^{2+}-SO_4^{2-} < Zn^{2+}-SO_4^{2-}$, $Cd^{2+}-SO_4^{2-}$.

Acknowledgment. Financial support of the Hong Kong RGC Earmarked Grant (HKUST6042/01P) and the HKUST PDF grant is gratefully acknowledged.

References and Notes

(1) Richardson, C. B.; Span, J. F. *Aerosol Sci.* **1984**,*15*, 563.
(2) Cohen, M. D.; Flagan, R. C.; Seinfeld, J. H. *J. Phys. Chem*. **1987**, *91*, 4563.
(3) Cohen, M. D.; Flagan, R. C.; Seinfeld, J. H. *J. Phys. Chem*. **1987**, *91*, 4575
(4) Chan, C. K.; Flagan, R. C.; Seinfeld, J. H. *Atmos. Environ.* **1992**, *26*, 1661.
(5) Tang, I. N. Munkelwitz, *J. Geophys. Res.* **1994**, *99*, 18801.
(6) Ha, Z.; Chan, C. K. *Aerosol Sci. Technol.* **1999**, *31*, 154.
(7) Chan, C. K.; Ha, Z.; Choi, M. Y.*Atmos. Environ.* **2000**, *34*, 4795.
(8) Chan, C. K.; Flagan, R. C.; Seinfeld, J. H. *J. Am. Ceram. Soc*. **1998**, *81*, 646−648.
(9) Chan, C. K.; Liang, Z.; Zheng, J.; Clegg, S. L.; Brimblecombe, P. *Aerosol Sci. Technol*. **1997**, *27*, 324.
(10) Liang Z.; Chan, C. K. *Aerosol Sci. Technol*. **1997**, *26*, 255.
(11) Zhang, Y. H.; Chan, C. K. *J. Phys. Chem. A* **2000**, *104*, 9191.
(12) Withmore, D. H. *J. Cryst. Growth* **1977**, *39*, 160.
(13) Frech, R.; Cazzanelli, E. *Solid State Ionics* **1983**, *9 & 10*, 95.
(14) Chulz, H.; Zucker, V.; Frech, R. *Acta Crystallogr., Sect. B* **1985**, *42*, 21.
(15) Brown, P. G. M.; Prue, J. E. *Proc. R. Soc. A.* **1955**, *232*, 320.
(16) Nair, V. S. K.; Nancollas, G. H. *J. Chem. Soc*. **1958**, 3706.
(17) Eigen, M.; Tamm, K. *Z. Elektrochem*. **1962**, *66*, 107.
(18) Atkinson, G.; Pstriucci, S. *J. Phys. Chem*. **1966**, *70*, 3122.
(19) Marshall, W. L. *J. Phys. Chem*. **1967**, *71*, 3584.
(20) (a). Rudolph, W. W. *Ber. Bunsen-Ges. Phys. Chem*. **1998**, *102*, 183. (b). Rudolph, W. W. *J. Chem. Soc., Faraday Trans*. **1998**, *94*, 989.
(21) Rull, F.; Balarew, Ch.; Alvarez, J. L.; Sobron, F.; Rodriguez, A. *J. Raman Spectrosc*. **1994**, *25*, 933.
(22) Nakamoto, K.; Fujuta, J.; Tanaka, S.; Kobayashi, M. *J. Am. Chem. Soc*. **1957**, *79*, 4904.
(23) Barraclough, C. G.; Tobe, M. L. *J. Chem. Soc*. **1961**, 1993.
(24) Eskenazi, R.; Rasovan, J.; Levitus, R. *J. Inorg. Nucl. Chem*. **1966**, *28*, 521.
(25) Finholt, J. E.; Anderson, R. W.; Fyfe, J. A.; Caulton, K. G. *Inorg. Chem*. **1965**, *4*, 43.
(26) Horn, R. W.; Weissberger, E.; Collman, J. P. *Inorg. Chem*. **1970**, *9*, 2367.
(27) Davis, A. R.; Oliver, B. G. *J. Phys. Chem*. **1973**, *77*, 1315.
(28) Chatterjee, R. M.; Adams, W. A.; Davis, A. R. *J. Phys. Chem*. **1974**, *78*, 246.
(29) Pye, C. C.; Rudolph, W. W. *J. Phys. Chem. A*. **1998**, *102*, 9933.
(30) Rull, F.; Prieto, M.; Sobron, E. *J. Phys.* **1994**, *IV.4 C2*, 47.
(31) Rull, F. *Z. Naturforsch. A* **1995**, *50*, 292.
(32) Rudolph, W. W.; Schoenher, S. *Z. Phys. Chem. (Munich)* **1991**, *31*, 172.
(33) Rudolph, W. W.; Brooker, M. H.; Tremaine, P. *J. Solution Chem*. **1997**, *26*,757.
(34) Rudolph, W. W.; Irmer, G. *J. Solution Chem*. **1994**, *23*, 663.
(35) Rudolph, W. W.; Pye, C. C. *J. Phys. Chem. B*, **1998**, *102*, 3564.
(36) Daly, F. P.; Brown, C. W.; Kester, D. R. *J. Phys. Chem*. **1972**, *76*, 3664.
(37) Fedorov, V. A.; Chernikova, G. E.; Kalosh, T. N.; Mironov, V. E. *Zh. Neorg. Khim*. **1971**, *16*, 170(E).
(38) Fedorov, V. A.; Chernikova, G. E.; Kunznechikhina, M. A.; Mironov, V. E. *Zh. Neorg. Khim*. **1973**, *18*, 337(E).
(39) Tang, I. N.; Fung, K. H.; Imre, D. G.; Munkelwitz, H. R. *Aerosol Sci. Technol*. **1995**, *23*, 443.
(40) Tang, I. N.; Fung, K. H. *J. Chem. Phys*. **1997**, *106*, 1653.
(41) Davis, E. J. *Aerosol Sci. Technol*. **1997**, *26*, 212.
(42) Buehler, M. F.; Allen, T. M.; Davis, E. J. *J. Colloid Interface Sci*. **1991**, *146*, 79.
(43) Foss, W.; Li, W.; Allen, T. M.; Blair, D. S.; Davis, E. *J. Aerosol Sci. Technol*. **1993**, *18*, 187.
(44) Rassat, S. D.; Davis E. J. *J. Aerosol Sci*. **1992**, *23*, 165.

(45) Schweiger, G. In *Analytical Chemistry of Aerosols*; Spurny, K. R., Ed., CRC Press: Boca Raton, 1999; pp 319−352.
(46) (a) Clegg, S. L.; Pitzer, K. S. *J. Phys. Chem*. **1992**, *96*, 3513. (b) Rard, J. A.; Miller, D. G. *J. Chem. Eng. Data* **1981**, *26*, 33−42.
(47) Ruben, H. W.; Templeton, D. H.; Rosenstein, R. D.; Olovsson, I. *J. Am. Chem. Soc*. **1961**, *83*, 820.
(48) Levy, H. A.; Lisensky, G. C. *Acta Crystallogr*. **1978**, *B34*, 3502.
(49) Palinkas, G.; Piccaluga, G.; Pinna, G.; Magini, M. *Chem Phys. Lett*. **1980**, *98*, 157.
(50) Matwiyoff, N. M.; Taube, H. *J. Am. Chem. Soc*. **1968**, *90*, 2796.
(51) Caminiti, R.; Licheri, G.; Piccaluga, G. *J. Appl. Crystallogr*. **1972**, *12*, 34.
(52) Broul, M.; Nyvlt, J.; Sohnel, O. *Solubility in Organic Two-component Systems*; Elsevier Scientific Publishing Company: New York, 1981; p 560.
(53) Lide, D. R. *Handbook of Chemistry and Physics*, 81st ed.; CRS Press: Boca Raton, 2000−2001; pp 15−26.
(54) (a) Rudolph, W. W.; Brooker, M. H.; Tremaine, P. *Z. Phys. Chem., Bd*. **1999**, *209*, S. 181. (b). Hayes, A. C.; Kruus, P.; Adams, W. A. *J. Solution Chem*. **1984**, *13*, 61.
(55) Nomura, H.; Shinobu, K.; Miyahara, Y. In *Water Metal Cations in Biological System*; Pullman, B., Yaji, K., Eds.; Japan Science Society Press: Tokyo, 1980; pp 31−46.
(56) Hayes, A. C.; Kruus, P.; Adams, W. A. *J. Solution Chem*. **1984**, *13*, 61
(57) Cieekes, J. M. T. M. *Z. Phys. Chem*. **1966**, *50*, 78.
(58) Lanier, R. D. *J. Phys. Chem*. **1966**, *70*, 3122.
(59) Butler, J. N.; Hsu, P. T.; Synnott, J. C. *J. Phys. Chem*. **1967**, *71*, 910.
(60) Buchner, R.; Capewll, S. G.; Hefter, G.; May, P. M. *J. Phys. Chem. B* **1999**, *103*, 1185.
(61) Butler, J. N.; Huston, R. *J. Phys. Chem*. **1970**, *74*, 2967.
(62) Luts, P.; Vanhees, J. L. C.; Yperman, J. H. E.; Mullens, J. M. A.; Poucke, L. C. Van. *J. Solution Chem*. **1992**, *21*, 375.
(63) Daly, F. P.; Brown, C. W.; Kester, D. R. *J. Phys. Chem*. **1972**, *76*, 3664.
(64) Rull, F.; Sobron, F.; Nielsen, O. F. *J. Raman Spectrosc*. **1995**, *26*, 663.
(65) Phillips, C. G.; Williams, R. J. P. *Inorganic Chemistry*; Clarendon Press: NewYork, 1965; Vol. 1, p 161.
(66) Vizcayno, C.; Garcia-Gonzalez, M. T. *Acta Crystallogr*. **1999**, *C55*, 8.
(67) (a) Dagnall, S. P.; Hague, D. N.; Towl, A. D. C. *J. Chem. Soc., Faraday Trans. II* **1982**, 2161. (b) Ohtaki, H.; Yamaguchi, T.; Maeda, M. *Bull. Chem. Soc. Jpn*. **1976**, *49*, 701.
(68) (a) Gupta, M. P.; Agrawal, J. L. *Acta Crystallogr*. **1977**, *C6*, 103. (b) Broomhead, J. M.; Nicol, A. D. I. *Acta Crystallogr*. **1948**, *1*, 88. (c) Cariati, F.; Erre, L.; Micera, G.; Panzanelli, A.; Ciani, G.; Sironi, A. *Inorg. Chim. Acta* **1983**, *80*, 57. (d) Bol, W.; Gerrits, G. J. A.; Panthaleon van Eck, C. L. *J. Appl. Crystallogr*. **1970**, *3*, 486. (e) Farnsworth, M. *Zinc Chemicals*; Zinc Institute: New York, 1973; pp 152−160.
(69) (a) Prince, R. H. In *Comprehensive Coordination Chemistry*; Wilkinson, G., Gillard, R. D., McCleverty, J. A., Eds.; Pergamon: New York, 1987; Vol. 1, pp 926−1004. (b) Ohtaki, H.; Maeda, M.; Ito, S. *Bull. Chem. Soc. Jpn*. **1974**, *47*, 2217. (c) Shapovalov, I. M.; Radchenko, I. V. *Russ. J. Struct. Chem*. **1971**, *12*, 705. (d) Ohtomo, N.; Arakawa, K. *Bull. Chem. Soc. Jpn*. **1980**, *53*, 1789. (e) Waizumi, K.; Tamura, Y.; Masuda, H.; Ohtaki, H. *Z. Naturforsch*. **1991**, *A46*, 307.